Complexes with Platinum−Ruthenium Bonds: Synthesis, Structure, and Fluxionality of Pt_3Ru Cluster Complexes

Brian T. Sterenberg, Michael C. Jennings, and Richard J. Puddephatt*

Department of Chemistry, University of Western Ontario, London Ontario, Canada N6A 5B7

Received May 3, 1999

The reaction of $[Pt_3(\mu_3\text{-CO})(\mu\text{-dppm})_3][PF_6]_2$, **1**, dppm = $Ph_2PCH_2PPh_2$, with $[HRu(CO)_4]^-$ initially gives $[Pt_3(\mu\text{-H})(\mu\text{-dppm})_3\{Ru(CO)_4\}]^+$, **2**, which contains a $PtRu(\mu\text{-H})$ unit. In solution, complex **2** rearranges to the cluster $[Pt_3Ru(\mu\text{-H})(CO)_2(\mu\text{-CO})_2(\mu\text{-dppm})_3]^+$, **3**, which has been characterized by X-ray structure determination to have a butterfly structure with ruthenium at a wingtip position and which contains a $Pt_2(\mu\text{-H})$ unit. Both complexes **2** and **3** exhibit fluxionality, which is defined by low-temperature NMR studies.

Introduction

Mixed metal cluster complexes of platinum are of interest because of their potential to act as models for mixed metal catalysts.[1] In particular, clusters that combine platinum with other metals have received considerable attention because they can model some of the structural and reactivity properties of the important bimetallic platinum alloy catalysts that are used in petroleum reforming.[2] A successful approach to the synthesis of cluster complexes containing Pt_3M units is to react the triplatinum cluster complex $[Pt_3(\mu_3\text{-CO})(\mu\text{-dppm})_3][PF_6]_2$ with metal carbonyl anions such as $[Ir(CO)_4]^-$ or $[Re(CO)_5]^-$.[3] The synthesis and subsequent reaction chemistry of Pt_3Ir cluster complexes prepared in this way are shown in Scheme 1.

This paper describes the synthesis and properties of two Pt_3Ru cluster complexes formed by reaction of **1** with the anion $[RuH(CO)_4]^-$. This combination of platinum and ruthenium in cluster complexes is of interest since larger platinum−ruthenium clusters have been shown to be useful homogeneous catalysts[4] and since they may act as partial models for heterogeneous bimetallic Pt/Ru catalysts.[2,5] In particular, platinum electrodes with ruthenium deposited on the surface have been the most successful catalysts for methanol oxidation in fuel cells.[5] In a more fundamental sense, there is still an incomplete understanding of the relationship of skeletal structure to electron count in heterometallic Pt−M cluster complexes as illustrated for tetranuclear Pt_nRu_{4-n} clusters in Table 1. With some exceptions and

Scheme 1

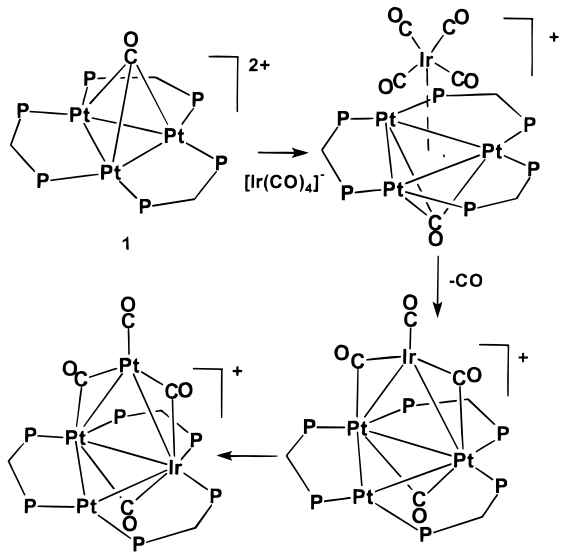

complications,[6] the skeletal structures of homonuclear Ru_4 clusters are those predicted by PSEPT theory, but the clusters containing platinum atoms tend to have lower electron counts since platinum atoms may not use all available orbitals in bonding.[7] Table 1 shows that, for a given skeletal structure, there is a general decrease in electron count as the value of n in the Pt_nRu_{4-n} cluster increases. However, while many Ru_4,[6] Ru_3Pt,[8] and Pt_4 clusters[7,9] are known, there are gaps in the database since few Pt_2Ru_2 clusters[10] and no Pt_3Ru

(1) (a) Farrugia, L. J. *Adv. Organomet. Chem.* **1990**, *31*, 301. (b) The Chemistry of Heteronuclear Clusters and Multimetallic Catalysts; Adams, R. D., Herrmann, W. A., Eds. *Polyhedron* **1988**, *7*, 2251−2462.
(2) (a) Guczi, L. *Metal Clusters in Catalysis*; Gates, B. C., Guczi, L., Knozinger, H., Eds.; Elsevier: New York, 1986. (b) Sinfelt, J. H. *Bimetallic Catalysts: Discoveries, Concepts and Applications;* Wiley: New York, 1983. (c) Xiao, J.; Puddephatt, R. J. *Coord. Chem. Rev.* **1995**, *143*, 457.
(3) (a) Spivak, G. J.; Yap, G. P. A.; Puddephatt, R. J. *Polyhedron* **1997**, *16*, 3861. (b) Sterenberg, B. T.; Spivak, G. J.; Yap, G. P. A.; Puddephatt, R. J. *Organometallics* **1998**, *17*, 2433. (c) Xiao, J.; Kristof, E.; Vittal, J. J.; Puddephatt, R. J. *J. Organomet. Chem.* **1995**, *490*, 1. (d) Xiao, J.; Hao, L.; Puddephatt, R. J.; Manojlovic-Muir, Lj.; Muir, K. W.; Torabi, A. A. *Organometallics* **1995**, *14*, 4183.
(4) Adams, R. D.; Barnard, T. S. *Organometallics* **1998**, *17*, 2567.
(5) Lee, C. E.; Bergens, S. H. *J. Phys. Chem. B* **1998**, *102*, 193.
(6) Pomeroy, R. K. In *Comprehensive Organometallic Chemistry*; Abel, E. W., Stone, F. G. A., Wilkinson, G., Eds.; Elsevier: Oxford, 1995; Vol. 7, Chapter 15.
(7) Mingos, D. M. P.; Wales, D. J. *Introduction to Cluster Chemistry*; Prentice Hall: Englewood Cliffs, NJ, 1990.
(8) (a) Powell, J.; Brewer, J. C.; Gulia, G.; Sawyer, J. F. *Inorg. Chem.* **1989**, *28*, 4470. (b) Farrugia, L. J.; McDonald, N.; Peacock, R. D. *J. Cluster Sci.* **1994**, *5*, 341. (c) Adams, R. D.; Li, Z.; Lii, J.-C.; Wu, W. *Inorg. Chem.* **1992**, *31*, 3445. (d) Adams, R. D.; Lii, J.-C.; Wu, W. *J. Cluster Sci.* **1993**, *4*, 423. (e) Ellis, D.; Farrugia, L. J.; Wiegeleben, P.; Crossley, J. G.; Orpen, A. G.; Walker, P. N. *Organometallics* **1995**, *14*, 481.
(9) (a) Imhof, D.; Venanzi, L. M. *Chem. Soc. Rev.* **1994**, 185. (b) Hao, L.; Vittal, J. J.; Puddephatt, R. J. *J. Chem. Soc., Chem. Commun.* **1995**, 2381.

10.1021/om990325s CCC: $18.00
Publication on Web 08/08/1999

Table 1. Some Tetranuclear Carbonyl Clusters of Platinum and Ruthenium

Ru_4 cluster	$PtRu_3$ cluster	Pt_2Ru_2 cluster	Pt_4 cluster
$[Ru_4(\mu\text{-H})_4(CO)_{12}]$	$[PtRu_3(\mu\text{-H})(\mu\text{-PR}_2)(CO)_9(PR_3)]$		$[Pt_4(\mu\text{-CO})_2L_4(ReO_4)_2]$
60 electron	58 electron		54 electron
tetrahedral	tetrahedral		tetrahedral
$[Ru_4(\mu\text{-H})(\mu_4\text{-C})(CO)_{12}]^-$	$[PtRu_3(\mu\text{-H})_2(CO)_{10}(cod)]$		$[Pt_4H(CO)(\mu\text{-CO})_3L_4]^+$
62 electron	60 electron		56 electron
butterfly	tetrahedral		tetrahedral
$[Ru_4(\mu\text{-PR}_2)_2(CO)_{13}]$	$[PtRu_3(CO)_{11}(PR_3)_2]$		$[Pt_4(\mu\text{-CO})_5L_4]$
64 electron	60 electron		58 electron
flat butterfly*	flat butterfly		butterfly
$[Ru_4(\mu\text{-Br})_2\{\mu\text{-P}(C_6H_4)\text{-PhCH}_2\text{PPh}_2\}_2(CO)_{13}]$	$[PtRu_3(\mu\text{-H})(\mu_4\text{-CCR})(CO)_9(PR_3)_2]$	$[Pt_2Ru_2(\mu\text{-H})_2(\mu_4\text{-C})(CO)_2(Cp)_2(PR_3)_2]$	
66 electron	62 electron	60 electron	
chain	spiked triangle	square	

Scheme 2

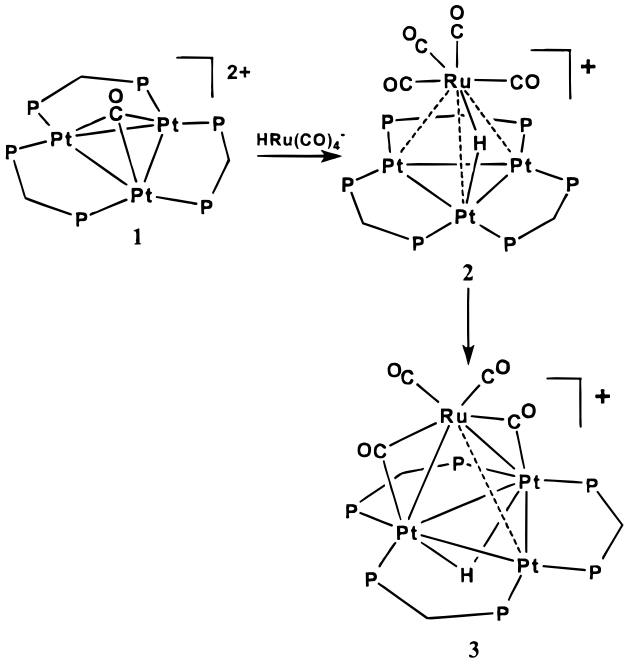

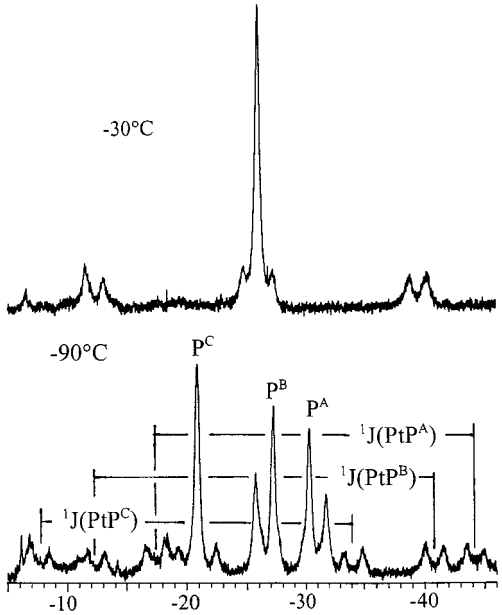

Figure 1. ^{31}P NMR spectrum of **2** at −30 °C (top) and −90 °C (bottom).

clusters have been reported.[11] The Pt_3Ru complexes reported below are thus the first examples of such complexes.

Results

Formation of $[Pt_3Ru(\mu\text{-H})(CO)_4(\mu\text{-dppm})_3][PF_6]$, 2. The reaction of $[Pt_3(\mu_3\text{-CO})(\mu\text{-dppm})_3]^{2+}$ with $[HRu(CO)_4]^-$ at low temperature occurred with a color change from orange to dark brown to give the cluster $[Pt_3Ru(\mu\text{-H})(CO)_4(\mu\text{-dppm})_2]^+$, **2**, as shown in Scheme 2. Complex **2** is formed cleanly at low temperature, but it is thermally unstable in solution, and at room temperature, it rearranged within hours to the isomeric cluster cation **3** (Scheme 2). Complex **2** could be isolated from its solution in dichloromethane by removal of the solvent at temperatures below −60 °C, and it was stable at room temperature in the solid state, but no further purification could be carried out without decomposition and attempts to grow crystals at low temperature were unsuccessful. The cluster cation **2** was therefore characterized by its spectroscopic properties and, in particular, by IR and variable-temperature NMR spectroscopy.

The NMR spectra of **2** were temperature dependent, indicative of easy fluxionality, and the spectra are first described in the fast exchange region, which was reached at temperatures above about −30 °C. The ^{31}P NMR spectrum of **2** showed a singlet resonance at $\delta = -26.0$, indicating that all six phosphorus atoms are equivalent. There were satellite spectra due to coupling to platinum, and these showed the typical pattern for a $Pt_3(\mu\text{-dppm})_3$ unit with 3-fold symmetry (Figure 1).[3,12] The directly measured coupling constants were $^1J(PtP) = 3290$ Hz, $^2J(Pt-P) = 280$ Hz, and $^3J(PP) = 180$ Hz for this isomer. The ^1H NMR spectrum of the cluster complex **2** contained a resonance for the hydride ligand at $\delta = -10.88$, which appeared as an apparent quintet with relative intensities 1:4:7:4:1, thus indicating coupling to three equivalent platinum atoms.[3,12] The apparent coupling $^1J(PtH) = 168$ Hz. The ^1H NMR spectrum also shows two multiplets for the dppm methylene hydrogens, indicating that the environments on either side of the Pt_3 plane are different, so that the effective symmetry is C_{3v}. The ^{13}C NMR spectrum of **2**

(10) Davies, D. L.; Jeffrey, J. C.; Miguel, D.; Sherwood, P.; Stone, F. G. A. *J. Organomet. Chem.* **1990**, *383*, 463.

(11) Adams, R. D., Ed. *Comprehensive Organometallic Chemistry II*; Abel, E. W., Stone, F. G. A., Wilkinson, G., Eds.; Elsevier: Oxford, 1995; Vol. 10.

(12) (a) Puddephatt, R. J.; Manojlovic-Muir, Lj.; Muir, K. W. *Polyhedron* **1990**, *9*, 2767. (b) Lloyd, B. R.; Puddephatt, R. J. *J. Am. Chem. Soc.* **1985**, *107*, 7785.

Chart 1

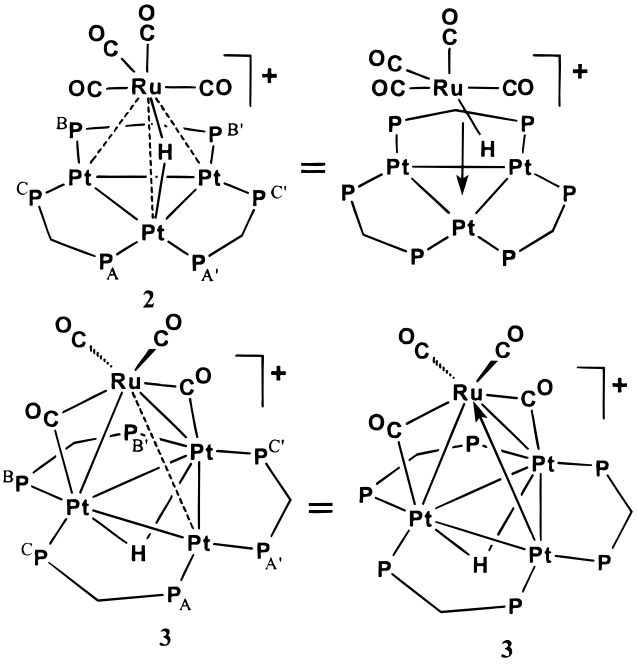

contained a single carbonyl resonance at $\delta = 203.5$, with no resolved ^{195}Pt satellite peaks, while the IR spectrum showed only terminal carbonyl stretches at ν(CO) = 2043, 1991, and 1960 cm^{-1}. These data show that all the carbonyl ligands are terminal and so are probably bound only to ruthenium.

While the above NMR data show that the effective symmetry of the cluster cation **2** above −30 °C is C_{3v}, the low-temperature NMR spectra show that the true symmetry is lower. At −90 °C, the ^{31}P NMR spectrum of **2** showed three resonances at $\delta = -20.9$ (P^C), −26.5 (P^B), and −31.0 (P^A), as shown in Figure 1 and with atom labeling shown in Chart 1. The true symmetry is thus C_s, and the mirror plane contains one platinum atom and bisects the other two (Chart 1). The coupling $^3J(P^AP^{B'}) = 180$ Hz is observed directly, while the corresponding coupling constant $^3J(P^CP^{C'})$ is observed only in the ^{195}Pt satellite spectra of the P^C resonance (Figure 1). Since these large values of ^3J(PP) are only observed when there is strong PtPt bonding, the data show that the Pt_3 triangle is still intact in **2**.[3,12] At −90 °C, the hydride resonance in the ^{1}H NMR spectrum appeared as a 1:4:1 triplet, with ^1J(PtH) = 470 Hz, showing that it is now coupled to only one platinum atom. The hydride must therefore lie in the mirror plane (Chart 1), and the fluxional process must lead to easy exchange of the hydride between platinum atoms. Thus, the coupling constant ^1J(PtH) = 470 Hz in the limiting low-temperature spectrum is almost 3 times the value of ^1J(PtH) = 168 Hz observed at higher temperatures. The magnitude of the coupling constant ^1J(PtH) = 470 Hz is smaller than is expected for a terminal platinum hydride, and although it is lower than the range of ^1J(PtH) = 559−627 Hz reported for PtRu(μ-H) groups in tetranuclear complexes,[8,9] it is much too high to be a longer range coupling since all reported values of such couplings are < 100 Hz.[8,9] The data indicate a relatively weak PtH bond in **2**, when compared to other PtRu(μ-H) groups.[8,9] At −90 °C, the carbonyl region of the ^{13}C NMR spectrum of **2** is very broad, but at −95 °C, three broad carbonyl resonances were resolved at $\delta = 206.5$, 203, and 198 with approximate intensity ratio 2:1:1, respectively. No couplings to ^{195}Pt were resolved, and the chemical shifts are all in the terminal carbonyl region. Thus, the $Ru(CO)_4$ group in **2** is indicated, but its stereochemistry is not rigorously defined. The activation energy for carbonyl fluxionality is approximately 33(1) kJ mol^{-1}, and this activation energy is less than for hydride fluxionality.

Because the carbonyl resonances in **2** were still broad at low temperature and did not unambiguously define the number of carbonyl ligands present, chemical evidence for the presence of four carbonyl ligands was sought. Thus, a spectroscopically pure sample of **2** was dissolved in CD_2Cl_2 and placed in an NMR tube that was then sealed. The complex rearranged cleanly to **3** over a period of several hours, with no detectable decomposition products formed and no release of free CO. Since cluster **3** is known to contain a total of four carbonyl ligands (see below) so must **2**.

The proposed structure for **2**, therefore, is shown in Scheme 2 and consists of three platinum atoms in a triangle with each edge bridged by a dppm ligand. The hydride ligand bridges between ruthenium and one of the platinum atoms, while the four carbonyl ligands are terminally bound to the ruthenium atom. The NMR data indicate the presence of strong Pt−Pt bonding in the Pt_3 triangle, but the nature of any direct Pt−Ru bonding is not defined. The stoichiometry of **2** shows that it is formed from **1** and $[RuH(CO)_4]^-$ with loss of the triply bridging carbonyl ligand from **1,** and hence it cannot be considered as a weak host−guest complex, as was proposed for the initial complex in the reaction of $[Ir(CO)_4]^-$ with **1** (Scheme 1).[3b] The electron count for the cluster **2** is 58, but Table 1 shows that there are not enough related clusters to be able to predict the skeletal structure of the cluster from this alone.[6−10]

The apparent 3-fold symmetry observed for **2** at higher temperatures is readily accounted for by a fluxional process in which the $[RuH(CO)_4]$ fragment rotates with respect to the Pt_3 triangle, such that the bridging hydride ligand remains bonded to ruthenium while it bridges sequentially to each of the three different platinum atoms, as shown in Scheme 3.

Isomerization of 2 to $[Pt_3Ru(\mu\text{-}H)(CO)_2(\mu\text{-}CO)_2(\mu\text{-dppm})_3][PF_6]$, 3. At room temperature in solution, complex **2** quickly and cleanly rearranges to the isomeric complex **3**, as shown in Scheme 2. Complex **3** forms very dark red-brown solutions which are thermally and air stable, and it readily forms very dark purple crystals. Although the isolated yield is low, conversion from **2** to **3** is essentially quantitative, as monitored by ^{31}P NMR spectroscopy. The low yield of the pure product results from decomposition during chromatography, which was necessary to separate **3** from the byproduct [PPN][PF_6].

The cluster complex **3** has been characterized both spectroscopically and by an X-ray structure determination. A diagram of the cation is shown in Figure 2, while crystal data and selected bond distances and angles are given in Tables 2 and 3. The Pt_3Ru core of **3** has a butterfly structure with the ruthenium atom at one of the wingtip positions. The hinge angle of 81.13(1)° is typical of butterfly clusters.[7] Each edge of the Pt_3 triangle is bridged by a dppm ligand, while the two Pt−

Scheme 3

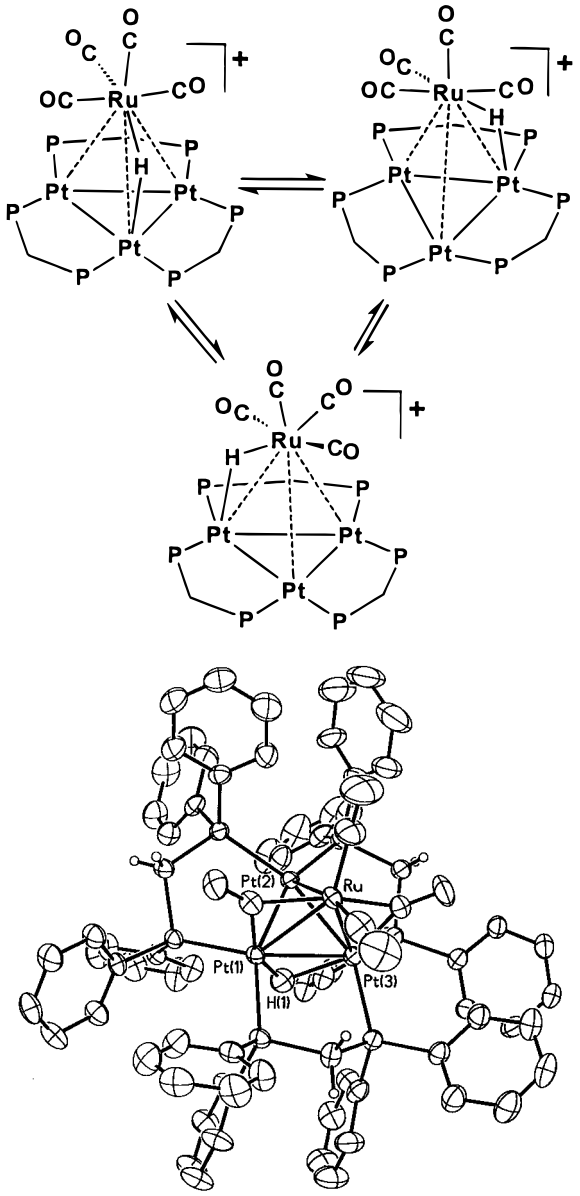

Figure 2. View of the cation $[Pt_3Ru(\mu\text{-}H)(CO)_2(\mu\text{-}CO)_2(\mu\text{-}dppm)_3]$, **3**. Thermal ellipsoids are drawn at 30% probability. Phenyl hydrogen atoms have been omitted for clarity.

Ru bonds are bridged by carbonyl ligands. Overall, in addition to its metal−metal bonds, the ruthenium atom is bonded to two terminal and two bridging carbonyl ligands. The conformations of the bridging dppm ligands are such that all phenyl substituents are equatorial on the ruthenium side of the Pt_3 plane and axial on the other side. This is clearly to accommodate the bulky $Ru(CO)_4$ group. In addition the atoms P(2) and P(5) are displaced well below the Pt_3 plane so that their equatorial phenyl substituents do not impinge on the bridging carbonyl ligands. The hydride ligand was located crystallographically and occupies a position bridging the atoms Pt(1) and Pt(3), on the opposite face from the ruthenium atom.

Although the Ru−Pt(2) distance of 2.9951(6) Å is considerably longer than the other Pt−Ru (2.7031(6), 2.7649(6) Å) and Pt−Pt distances (2.6128(3)−2.7286(3) Å), the presence of a weak metal−metal bond is not ruled out since platinum−ruthenium bonds as long as 2.990(6) Å have been observed in clusters.[13] The geometry at ruthenium suggests that a weak Ru−Pt(2) bond may be present, as discussed below. In addition to the metal−metal bonds and the bridging carbonyls, the ruthenium atom is bonded to two terminal carbonyls, one of which is approximately trans to the Ru−Pt(2) vector [C(40)−Ru−Pt(2) = 166.0(3)°], while the second is approximately coplanar with the Pt(3)Pt(1)Ru triangle. This geometry is reasonable if there is a Pt(2)Ru bond, but the terminal carbonyls would be expected to lie more symmetrically on either side of the Pt(1)Pt(3)Ru triangle if there were no Pt(2)Ru bond. Like **2**, complex **3** is a 58-electron cluster. If considered as a butterfly cluster with no Pt(2)−Ru bond, the hinge atoms Pt(1) and Pt(3) have 18-electron configurations, while the wingtip atoms Pt(2) and Ru have 16-electron configurations. The 16-electron configuration is common for platinum but not for ruthenium, and a dative bond from Pt(2) to Ru may then be favored to give ruthenium an 18-electron count (Chart 1). Of course, if this PtRu

Table 2. Crystal Data and Structure Refinement for $[Pt_3Ru(\mu\text{-}H)(CO)_2(\mu\text{-}CO)_2(\mu\text{-}dppm)_3][PF_6]\cdot CH_2Cl_2$ (3)

empirical formula	$C_{80}H_{69}Cl_2F_6O_4P_7Pt_3Ru$
fw	2182.45
temperature	293(2) K
wavelength	0.71073 Å
space group	$P2_1/n$
a	12.6881(3) Å
b	26.5007(4) Å
c	23.6364(5) Å
β	98.0317(8)°
volume	7869.6(3) Å^3
Z	4
density (calcd)	1.841 Mg/m^3
absorption coefficient	5.778 mm^{-1}
no. of indep reflns	16026 [R(int) = 0.0460]
absorption correction	Scalepack
no. of data/restraints/params	16026/0/928
goodness-of-fit on F^2	1.027
final R indices [$I>2\sigma(I)$]	R1 = 0.0397, wR2 = 0.0930
R indices (all data)	R1 = 0.0578, wR2 = 0.1035
largest diff peak and hole	1.277 and −0.870 e Å^{-3}

Table 3. Selected Bond Lengths [Å] and Angles [deg] for $[Pt_3Ru(\mu\text{-}H)(CO)_2(\mu\text{-}CO)_2(\mu\text{-}dppm)_3][PF_6]\cdot CH_2Cl_2$ (3)

Pt(1)−C(10)	2.090(7)	Pt(3)−P(6)	2.349(2)
Pt(1)−P(2)	2.283(2)	Pt(3)−Ru	2.7649(6)
Pt(1)−P(1)	2.328(2)	Pt(3)−H(1)	1.99(7)
Pt(1)−Pt(2)	2.6128(3)	Ru−C(40)	1.82(1)
Pt(1)−Ru	2.7031(6)	Ru−C(30)	1.86(1)
Pt(1)−Pt(3)	2.7286(3)	Ru−C(20)	2.063(7)
Pt(2)−P(3)	2.270(2)	Ru−C(10)	2.073(7)
Pt(1)−H(1)	1.75(7)	C(10)−O(10)	1.171(8)
Pt(2)−P(4)	2.273(2)	C(20)−O(20)	1.183(8)
Pt(2)−Pt(3)	2.6216(3)	C(30)−O(30)	1.14(1)
Pt(2)−Ru	2.9951(6)	C(40)−O(40)	1.19(1)
Pt(3)−C(20)	2.109(8)		
Pt(3)−P(5)	2.296(2)		

Pt(2)−Pt(1)−Ru	68.56(1)	Pt(2)−Pt(3)−Ru	67.50(1)
Pt(2)−Pt(1)−Pt(3)	58.739(9)	Pt(1)−Pt(3)−Ru	58.95(1)
Ru−Pt(1)−Pt(3)	61.20(1)	Pt(1)−Ru−Pt(3)	59.86(1)
Pt(1)−Pt(2)−Pt(3)	62.837(9)	Pt(1)−Ru−Pt(2)	54.29(1)
Pt(1)−Pt(2)−Ru	57.15(1)	Pt(3)−Ru−Pt(2)	53.97(1)
Pt(3)−Pt(2)−Ru	58.53(1)		
Pt(2)−Pt(3)−Pt(1)	58.425(9)		

(13) Adams, R. D.; Barnard, T. S.; Li, Z.; Wu, W.; Yamamoto, J. *Organometallics* **1994**, *13*, 2357.

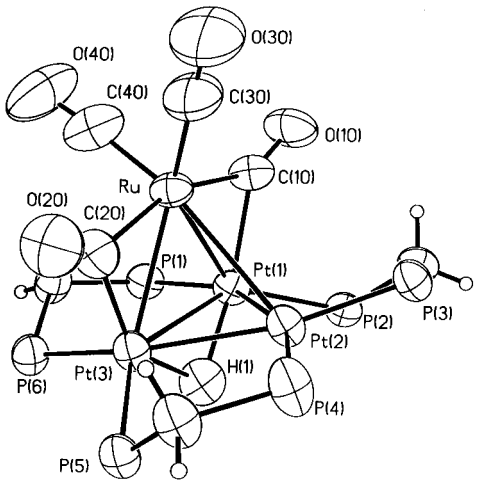

Figure 3. View of the core atoms of the cation of **3**. Thermal ellipsoids are shown at 50% probability.

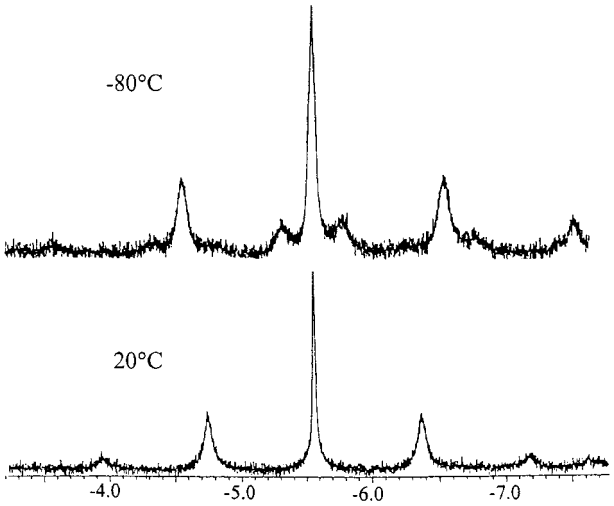

Figure 4. ^{1}H NMR spectrum of the hydride region of **3** at 20 °C (top) and −80 °C (bottom).

bond is present, the cluster might be described as a distorted tetrahedron rather than a butterfly.

The cluster **3** is fluxional, and so its NMR spectra are temperature dependent. At room temperature, the ^{31}P NMR spectrum of **3** showed one very broad peak at $\delta = -11$, indicating that it is an intermediate exchange rate region of fluxionality. In the ^{1}H NMR spectrum, the hydride resonance appeared at $\delta = -5.56$ as a 1:4:7:4:1 quintet, indicating coupling to three effectively equivalent platinum atoms (Figure 4). The averaged coupling constant $^{1}J(\mathrm{PtH}) = 486$ Hz was observed. The resonances due to the $CH^{a}H^{b}P_2$ protons were broad and unresolved. The ^{13}C NMR of **3** contained two peaks at $\delta = 198.7$ and 261.5, corresponding to bridging and terminal carbonyl ligands, respectively. The bridging carbonyl signal showed satellite spectra due to coupling to ^{195}Pt, with the observed coupling $^{1}J(\mathrm{PtC}) = 140$ Hz, but the satellites were broad and poorly resolved due to the intermediate rate of fluxionality. The terminal carbonyl resonance showed a coupling $^{2}J(\mathrm{PtC}) = 28$ Hz.

At −80 °C, the ^{31}P NMR spectrum of **3** contained three resonances at $\delta = -5.6$ (P^{A}), −8.6 (P^{B}), and −20.5 (P^{C}), with a large coupling $^{3}J(P^{A}P^{B'}) = 200$ Hz (see Chart 1 for atom labeling) as well as the expected satellite spectra due to $^{1}J(\mathrm{PtP})$ coupling. The hydride resonance

Scheme 4

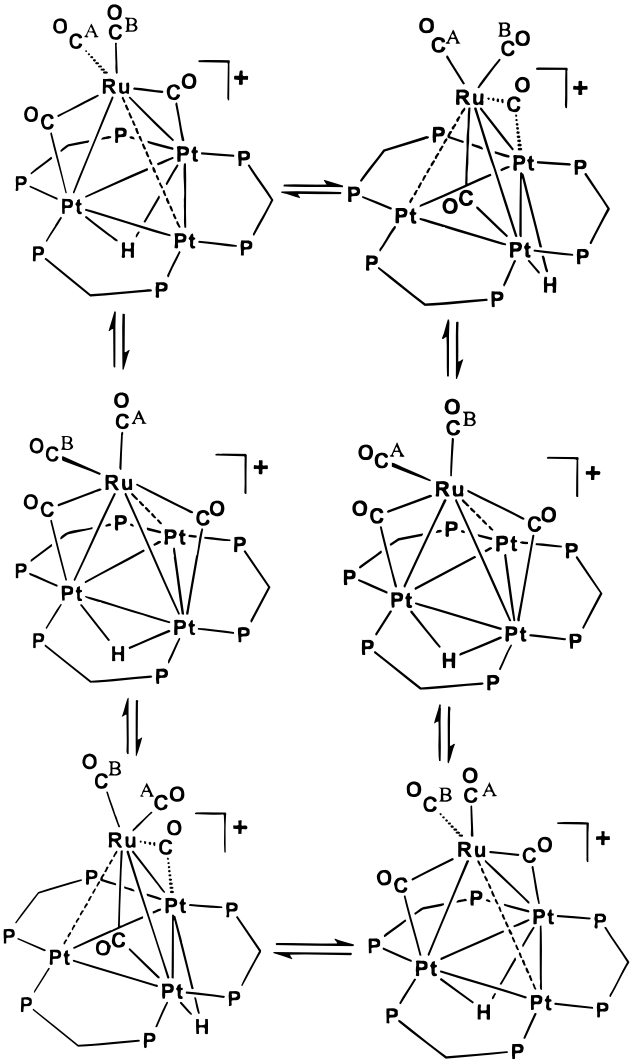

in the ^{1}H NMR spectrum at −80 °C appeared as a 1:8:18:8:1 quintet of 1:4:1 triplets due to the couplings $^{1}J(\mathrm{PtH}) = 645$ Hz to two equivalent platinum atoms and the coupling $^{2}J(\mathrm{PtH}) = 156$ Hz to one platinum atom (Figure 4). The observed coupling at room temperature of $J(\mathrm{PtH}) = 470$ Hz (Figure 4) is very close to the weighted average of these coupling constants [$2/3 \times 645 + 1/3 \times 156 = 473$ Hz]. The hydride ligand thus occupies a position bridging the two equivalent platinum atoms at the hinge of the butterfly, in accordance with the X-ray structure determination. Note that the magnitude of $^{1}J(\mathrm{PtH})$ is greater in **3** than in **2** (645 and 470 Hz, respectively), indicating a stronger PtH bond in **3**. In the ^{13}C NMR spectrum at low temperature, the terminal carbonyl resonance splits into two separate but closely spaced peaks at $\delta = 198.6$ and 198.4, while the bridging carbonyl resonance remained unchanged except that the satellites due to the coupling $^{1}J(\mathrm{PtC}) = 456$ Hz were well resolved. Note that this coupling is nearly 3 times the value observed at room temperature, as expected if the bridging carbonyls migrate between platinum atoms in the fluxional process.

The fluxional process that accounts for the observed spectra is shown in Scheme 4. The $Ru(\mu\text{-}CO)_2(CO)_2$ unit alternately bridges the three Pt−Pt bonds, while the hydride ligand on the opposite side of the Pt_3 plane

moves in tandem such that it is always opposite the ruthenium atom. This process leads to effective 3-fold symmetry for the complex, as exhibited in the room-temperature NMR spectra. The proposed windshield-wiper movement of the $Ru(CO)_4$ unit with respect to the Pt_3 triangle naturally leads to exchange of the two terminal carbonyl environments at each step, while two complete rotations are needed to give effectively equal coupling of each platinum atom to each bridging carbonyl carbon atom. Similar fluxional processes have been established previously for butterfly clusters.[3b,14]

If the fluxional processes of the two clusters are compared, there is a much higher barrier in **3** than in **2**. Thus approximate activation energies at the coalescence temperatures, as determined using the Eyring equation, were $\Delta G^* = 49(1)$ kJ mol^{-1} for **3** at approximately 0 °C and 37(1) kJ mol^{-1} for **2** at approximately −60 °C (^{31}P NMR). Since steric effects are likely to be about the same in each isomer, this difference probably arises from bonding effects. In the mechanisms proposed for fluxionality (Schemes 3 and 4), the hydride ligand (and the ruthenium atom) migrates between metal atoms in each case, but only for **3** do the bridging carbonyls do so. The difference in activation energies is then probably associated with the making and breaking of PtC bonds during fluxionality of **3**.

Discussion

The reaction of $[Pt_3(\mu_3\text{-}CO)(\mu\text{-}dppm)_3][PF_6]_2$ with [PPN][$HRu(CO)_4$] occurs in two steps to give first a complex **2** containing a $PtRu(\mu\text{-}H)$ group, which rearranges easily to an isomer **3** containing a $Pt_2(\mu\text{-}H)$ group. In cluster **2**, it is likely that the two components which may be considered as $[Pt_3(\mu\text{-}dppm)_3]^{2+}$ and $[RuH(CO)_4]^-$ are relatively weakly bound. The evidence for this is the low value of the coupling constant ^1J(PtH), the significantly greater ease of fluxionality in **2** compared to **3**, the absence of bridging carbonyl ligands, and very easy fluxionality of the carbonyl ligands in **2**. An even more weakly bound intermediate is formed in the reaction of **1** with $[Ir(CO)_4]^-$ (Scheme 1), and this primary adduct also exhibits easier fluxionality, which causes all carbonyls to appear equivalent even at −90 °C.[3] The increased stability of the initial Pt_3Ru complex **2** probably results from the presence of the hydride ligand which forms a bridge bond to one of the platinum atoms that is at least strong enough to cause dissociation of the triply bridging carbonyl ligand from **1**. There could also be donation of electron density from ruthenium to the center of the Pt_3 unit. It should be noted that, although the second step of the reaction sequences in Schemes 1 and 2 both lead to a butterfly cluster complex with iridium or ruthenium in a wingtip position, the reactions are different in nature and so there is no reason to expect them to have similar rates. In Scheme 1, this reaction involves loss of a carbonyl ligand from iridium, whereas in Scheme 2 it involves migration of the hydride ligand, perhaps by tunneling through the Pt_3 triangle.

There are now several tetranuclear cluster complexes containing the $Pt_3(\mu\text{-}dppm)_3$ unit, with the fourth metal M ranging from group 7 to 14, and a selection of those having tetrahedral or butterfly structures is shown in Chart 2.[3,12,14,15] The series is one of the most extensive known for related heteronuclear clusters, with M ranging from mid-transition metals such as rhenium to main group metals such as tin. For clusters such as $[Pt_3(\mu\text{-}dppm)_3(SnX_3)]^+$, the clusters are often considered as trinuclear with SnX_3^- acting as a two-electron ligand, but the system in Chart 2 is useful for comparison purposes. If M is from groups 8−10, there is a tendency to form 58-electron butterfly clusters, but on either side, there is a tendency to form tetrahedral clusters with 54- to 58-electron counts. The only 56-electron butterfly cluster in the series is the rhenium derivative $[Pt_3(\mu\text{-}dppm)_3\{Re(CO)_3L\}]^+$, which is known with several neutral ligands L.[3]

With respect to butterfly clusters in the series containing Pt_nRu_{4-n} cores (Table 1), complex **3** is the first known for $n = 3$ and there is no known example for $n = 2$. A comparative sequence might include $[Ru_4(\mu\text{-}H)(\mu_4\text{-}C)(CO)_{12}]^-$ (62-electron); $[PtRu_3(CO)_{11}(PCy_3)_2]$ (60-electron); $[Pt_3Ru(\mu\text{-}H)(CO)_2(\mu\text{-}CO)_2(\mu\text{-}dppm)_3]^+$ (58-electron); $[Pt_4(\mu\text{-}CO)_5(PR_3)_4]$ (58-electron). It could be argued that an isomer of **3** with ruthenium at the hinge position and platinum atoms at both wingtip positions should be more stable, but it has not been possible to synthesize such a complex from **3**, even by heating in solution (cf. Scheme 1).[3]

Experimental Section

Infrared spectra were recorded as Nujol mulls or as solutions in CH_2Cl_2 by using a Perkin-Elmer 2000 FTIR spectrometer. The ^{1}H, ^{31}P{^{1}H}, and ^{13}C{^{1}H} NMR spectra were recorded using a Varian Gemini 300 NMR spectrometer with CD_2Cl_2 as solvent. Approximate activation energies for fluxionality were obtained by using the Eyring equation at the coalescence temperature. The compounds $[Pt_3(\mu_3\text{-}CO)(\mu\text{-}dppm)_3][PF_6]_2$ (**1**)[16] and [PPN][$HRu(CO)_4$][17] were prepared according to literature methods. All manipulations were carried out using standard Schlenk techniques under an atmosphere of prepurified argon.

$[Pt_3Ru(CO)_4(\mu\text{-}H)(\mu\text{-}dppm)_3][PF_6]$ (2). The compounds $[Pt_3(\mu_3\text{-}CO)(\mu\text{-}dppm)_3][PF_6]_2$ (**1**, 40 mg, 0.019 mmol) and PPN-[$HRu(CO)_4$] (15 mg, 0.019 mmol) were dissolved in CD_2Cl_2 (0.5 mL) at −80 °C, resulting in the formation of a dark brown solution of $[Pt_3Ru(\mu\text{-}H)(CO)_4(\mu\text{-}dppm)_3][PF_6]$ (**2**). NMR spectra of the resulting solution were recorded at −95, −90, −60, −30, and 20 °C. At room temperature in solution, **2** decomposes within hours to compound **3**. IR (CH_2Cl_2 solution): ν(CO) = 2043 s, 1991 s, 1960 s cm^{-1}. NMR in CD_2Cl_2 at 20 °C: δ(^{1}H) = 5.8 [b, 3H, CHP]; 4.8 [b, 3H, CHP]; −10.88 [1:4:7:4:1 multiplet, ^1J(PtH) = 168 Hz, PtH]. δ(^{31}P) = −26.0 [^1J(PtP) = 3290 Hz, ^2J(PtP) = 280 Hz, ^3J(PP) = 180 Hz, dppm]. δ(^{13}C) = 203.5 [s, CO]. NMR at −90 °C: δ(1H) = 5.7 [b, 2H, CHP]; 4.9 [b, 2H, CHP]; 4.1 [b, 1H, CHP]; 3.5 [b, 1H, ^3J(PtH) = 90 Hz, CHP]; −11.1 [^1J(PtH) = 470 Hz, PtH]. δ(^{31}P) = −20.9 [^1J(PtP) = 3230 Hz, ^2J(PtP) = 200 Hz, ^3J(P^{C}P$^{C'}$) = 180 Hz]; −26.5 [d, ^3J(PP) = 180 Hz, ^1J(PtP) = 3470 Hz]; −31.0 [^3J(PP) = 180 Hz, ^1J(PtP) = 3220 Hz]. δ(^{13}C) = 206.5 [s, 2C, CO]; 203 [s, 1C, CO], 198 [s, 1C, CO].

Isolation of $[Pt_3Ru(CO)_4(\mu\text{-}H)(\mu\text{-}dppm)_3][PF_6]$ (2) at Low Temperature. The cluster complex **2** was formed as

(14) Douglas, G.; Manojlovic-Muir, Lj.; Muir, K. W.; Jennings, M. C.; Lloyd, B. R.; Rashidi, M.; Schoettel, G.; Puddephatt, R. J. *Organometallics* **1991**, *10*, 3927.
(15) Jennings, M. C.; Schoettel, G.; Roy, S.; Puddephatt, R. J.; Douglas, G.; Manojlovic-Muir, Lj.; Muir, K. W. *Organometallics* **1991**, *10*, 580.
(16) Ferguson, G.; Lloyd, B. R.; Puddephatt, R. J. *Organometallics* **1986**, *5*, 344.
(17) Walker, H. W.; Ford, P. C. *J. Organomet. Chem.* **1981**, *214*, C43.

Chart 2

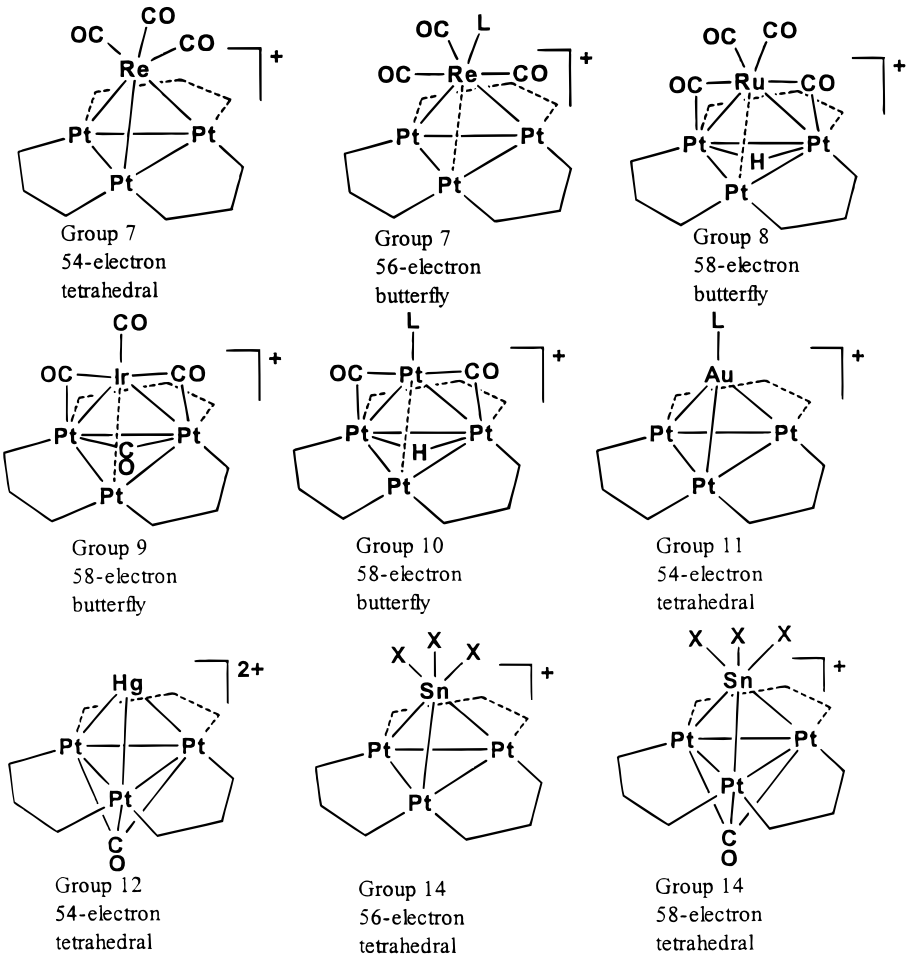

above by addition of CH_2Cl_2 (3 mL) to $[Pt_3(\mu_3\text{-CO})(\mu\text{-dppm})_3][PF_6]_2$ (**1**, 40 mg, 0.019 mmol) and PPN[$HRu(CO)_4$] (15 mg, 0.019 mmol) at −80 °C. The solvent was then removed in vacuo at −60 °C over a 5 h period. The resulting brown solid was left under dynamic vacuum for 24 h and then dissolved in CD_2Cl_2 (0.5 mL). The ^{31}P NMR spectrum confirmed the presence of **2** in near quantitative yield. The sample was then monitored by ^{31}P NMR and showed complete conversion to **3**.

$[Pt_3Ru(\mu\text{-H})(CO)_2(\mu\text{-CO})_2(\mu\text{-dppm})_3][PF_6]$ (3). Cluster complex **2** was prepared as above by dissolving $[Pt_3(\mu_3\text{-CO})(\mu\text{-dppm})_3][PF_6]_2$ (**1**, 195 mg, 0.095 mmol) and PPN[$HRu(CO)_4$] (71 mg, 0.095 mmol) in CH_2Cl_2 (20 mL) at −80 °C. The resulting dark brown solution was then allowed to warm to room temperature and allowed to stir for 4 h. The solvent was removed in vacuo, and the resulting dark brown residue was chromatographed (neutral alumina, 50:50 hexane/acetone). The dark red-brown fraction was collected, and the solvent was removed in vacuo. The residue was recrystallized from CH_2Cl_2/Et_2O and dried in vacuo. Yield: 70 mg, 35%. Anal. Calcd for $C_{79}H_{67}F_6O_4P_7Pt_3Ru$: C, 45.24; H, 3.22. Found: C, 45.51; H, 3.26. IR (Nujol mull): ν(CO) = 2007 s, 1940 s, 1807 w, 1779 s cm^{-1}. NMR in CD_2Cl_2 at 20 °C: $\delta(^1H)$ = 5.8 [b, 3H, CHP]; 4.8 [b, 3H, CHP]; −5.56 [m, ^1J(PtH) = 486 Hz, PtH]. $\delta(^{31}P)$ = −11 (vb, dppm). $\delta(^{13}C)$ = 198.7 [^2J(PtC) = 28 Hz, RuCO]; 261.5 [^1J(PtC) = 140 Hz, μ-CO]. NMR at −80 °C: $\delta(^1H)$ = 5.75 [b, 2H, CHP]; 5.0 [b, 2H, CHP]; 4.14 [b, 1H, CHP]; 3.45 [b, 1H, CHP]; −5.66 [m, ^1J(PtH) = 645 Hz, ^2J(PtH) = 156 Hz, $Pt_2(\mu$-H)]. $\delta(^{31}P)$ = −5.6 [d, ^3J(PP) = 200 Hz, ^{1}J(PtP) = 2980 Hz]; −8.6 (d, ^3J(PP) = 200 Hz, ^{1}J(PtP) = 2800 Hz]; −20.5 (s, ^1J(PtP) = 3630 Hz, ^2J(PtP) = 550 Hz, ^3J(PP) = 190 Hz]. $\delta(^{13}C)$ = 198.4 [s, RuCO]; 198.6 [s, RuCO]; 261.5 [^1J(PtC) = 456 Hz, μ-CO].

X-ray Structure Determination. Crystals of $[Pt_3Ru(\mu\text{-H})(CO)_2(\mu\text{-CO})_2(\mu\text{-dppm})_3][PF_6]\cdot CH_2Cl_2$ were grown by slow diffusion of pentane into a methylene chloride solution. A dark purple block was selected and mounted on a glass fiber. Data were collected at room temperature using a Nonius Kappa-CCD diffractometer with COLLECT (Nonius, 1998) software. The unit cell parameters were calculated and refined from the full data set. Crystal cell refinement and data reduction was carried out using the Nonius DENZO package. The data were scaled using SCALEPACK (Nonius, 1998), and no other absorption corrections were applied. The crystal data and refinement parameters are listed in Table 1. Selected interatomic distances and angles are listed in Table 2. The reflection data and systematic absences were consistent with the monoclinic space group $P2_1/n$.

The SHELXTL 5.03 (Sheldrick, G. M., Madison, WI) program package was used to solve the structure by direct methods and successive difference Fouriers. The refinement was unremarkable. All non-hydrogen atoms were refined with anisotropic thermal parameters. The metal hydride was located in the Fourier map and refined isotropically, while the positions of the other hydrogen atoms were calculated geometrically and rode on their respective carbon atoms. The solvent molecule refined satisfactorily. The largest residual electron density peak (1.277 e/A^3) was associated with one of the core metals. Full-matrix least-squares refinement on F^2 gave R1 = 3.97 and wR2 = 9.30 at convergence.

Acknowledgment. We thank NSERC (Canada) and PRF for financial support.

Supporting Information Available: Tables of X-ray data for complex **3**. This material is available free of charge via the Internet at http://pubs.acs.org.

OM990325S